Electric Power Systems Research 133 (2016) 198–208

Contents lists available at ScienceDirect

Electric Power Systems Research

journal homepage: www.elsevier.com/locate/epsr

Control methodology for compensation of grid voltage unbalance using a series-converter scheme for the DFIG

Vinicius P. Suppioni, Ahda P. Grilo*, Julio C. Teixeira

Centro de Engenharia, Modelagem e Ciências Sociais Aplicadas, Universidade Federal do ABC, Santo André, Brazil

ARTICLE INFO

Article history:
Received 2 October 2015
Received in revised form
22 December 2015
Accepted 23 December 2015

Doubly fed induction generator
Unbalanced grid voltage compensation
Symmetrical components
Torque control

ABSTRACT

This paper proposes a control methodology for compensation of grid voltage unbalances using a new scheme of doubly fed induction generator (DFIG) based on a series grid side converter (SGSC), the series-DFIG scheme. In such DFIG scheme, the grid side converter (GSC), which is usually connected in parallel to the machine stator, is replaced by the SGSC, connected in series with the machine stator. The proposed control methodology exploits the potential of the series-DFIG scheme to avoid that grid voltage unbalances compromise the machine operation, and to compensate voltage unbalances at the point of common coupling (PCC), preventing adverse effects on loads connected next to the PCC. This methodology uses the rotor side converter (RSC) to control the negative sequence current injected through the machine stator and the SGSC to control the negative sequence stator voltage to minimize the electromagnetic torque oscillations. The proposed control methodology is validated by simulation results.

1. Introduction

Wind power has become one important source of energy. Due to the characteristics of regions with good wind energy availability, wind turbines are frequently connected to power grids susceptible to unbalanced grid voltage conditions due to their placement in remote or rural areas. Unbalanced grid voltages are caused by different factors as: asymmetrical loads, transformer windings, asymmetrical transmission impedances and grid faults [1,2]. They are responsible for operation issues, such as electrical machine overheating, transformer overloading, and capacity limitation of power electronic devices. Such issues have encouraged the publication of standards and guidelines to limit the operation when voltage unbalances are present, as the one from the National Electrical Manufacturers Association (NEMA) in Standards Publication no. MG 1-1993 [3], which recommends the derating of asynchronous machines under voltage unbalances up to 5%, and does not recommend the operation above this limit.

In the past, as the penetration of wind power was very low, the wind turbine connection requirements were focused mainly on the turbine protection and, in case of disturbances, the wind turbines were simply disconnected from the grid. This scenario has changed and, currently, wind turbines should remain connected during system disturbances and, in some cases, wind turbines are required to actively support the grid. Among the possible disturbances, voltage unbalance is responsible for a poor wind generator performance and it is an important cause of partial or total disconnection of wind parks [4,5]. As a consequence, some strategies for the operation of wind turbines under unbalanced voltage conditions have already been proposed and are still evolving towards an effective solution.

Among the current technologies used for wind energy conversion, the Doubly Fed Induction Generator (DFIG) has been one of the most employed in the last years due to its operational flexibility. When this generator is subjected to even a small unbalanced grid voltage, it presents highly unbalanced stator and rotor currents [5]. These unbalanced currents are responsible for oscillations in the electromagnetic torque, compromising the machine integrity [6]. When the grid operation is analyzed, the unbalanced machine operation can increase the grid voltage unbalance level, once the machine presents low negative sequence impedance.

Several control strategies have already been proposed for DFIG operating under unbalanced voltage conditions. The most of them have focused on compensating the negative effects of grid unbalanced voltages on the generator operation [7–13]. Other strategies focus on improving the grid voltage unbalance levels by injecting a negative sequence current [1]. The objectives of the negative sequence current injection usually are: to reduce the unbalanced current flowing in the grid; to reduce the voltage unbalance at the

* Corresponding author. Tel.: +55 1149968293.
E-mail address: ahda.pavani@ufabc.edu.br (A.P. Grilo).

http://dx.doi.org/10.1016/j.epsr.2015.12.034

Point of Common Coupling (PCC); or to improve the whole grid voltage unbalance profile.

The natural solution for voltage unbalance compensation is to use the converters already present in DFIG for this task. In a conventional DFIG, the machine rotor is coupled to the grid by a bidirectional converter, which is composed by the Rotor Side Converter (RSC), the DC link and the Grid Side Converter (GSC). The RSC is connected to the rotor windings and the GSC is connected in parallel with the machine stator winding and the PCC.

As the rotor machine currents can be controlled by the RSC, such control can be used (a) to reduce the electromagnetic torque oscillations produced by the stator unbalanced voltages [8–17]; or (b) to inject a negative sequence current in the grid through the machine stator [1]. It is also possible to inject a negative sequence current by the GSC [1,18,19] which can be used either to compensate the machine own influence or to minimize the grid voltage unbalance, as long as there is a residual power available in the converter. A coordinated solution combining the RSC and GSC negative sequence controls [1,20,21] tends to be more efficient. However, the techniques using the conventional DFIG are limited by the remaining capacity of the converters, which depends on the point of operation of the generator.

Another solution to reduce the DFIG susceptibility to voltage disturbances has been developed [22], by inserting a third converter based on Dynamic Voltage Restorer (DVR) architecture. This solution allows the compensation of the machine stator voltage from any disturbance of the grid voltage. The third-converter, called Series Grid Side Converter (SGSC), is coupled by a series transformer to the machine terminals and shares the DC link with the GSC. In [23] an improved voltage ride through capability of this DFIG topology has been observed when compared to the traditional scheme. This configuration has also a better capability to deal with network unbalanced conditions [24].

In order to avoid the extra cost of a third converter, a two-converter series topology in which the SGSC replaces entirely the GSC functions, has been proposed [25–27]. To achieve this objective the DC-Link voltage control was integrated to the SGSC. This DFIG topology has allowed to combining the capacity to deal with voltage disturbances of the three-converter series topology with the lower cost of the two converters of a traditional DIFG scheme. It is worth to highlight that, compared to the conventional DFIG scheme, the series-DFIG presents a considerable higher potential to compensate the voltage unbalance at the PCC due its capacity to control the stator voltage.

Although the series compensation of the series-DFIG scheme can improve the voltage unbalance levels at the PCC, so far no control strategies have been proposed for this task using this scheme. This task requires a coordinated control of the converters to inject the negative sequence current and the compensation of the torque oscillations due to these currents in the machine. To accomplish this, the present study proposes the control of the negative sequence current by the RSC, and the control of the stator voltage by the SGSC to minimize the torque oscillations.

In this context, a control strategy to compensate grid unbalanced voltages using the series-DFIG scheme is developed in this paper. The contributions of the proposed control methodology are: (a) exploiting a new DFIG configuration, which presents the functions of a DVR without the need of an additional converter; (b) protecting the integrity of the machine under grid voltage unbalances conditions; (c) minimizing or even eliminating the grid voltage unbalance at the PCC, therefore preventing issues associated with loads connected to grid sensitive to voltage unbalances.

The paper is organized as follows: Section 2 provides the proposed configuration of the DFIG operation under unbalanced currents and the machine dynamic model which is used in Section 3 to show the proposed control methodology. The methodology is validated by simulation results presented in Section 4. Finally, in Section 5 the main conclusions are presented.

2. System architecture and model

The insertion of the SGSC as a third converter in the traditional DFIG topology has proved to improve the capacity of the DFIG to respond to voltage sags, swells and faults in the grid, since it enables controlling the stator terminal voltage by regulating the output voltage of SGSC [23]. When conventional parallel grid side converter is completely replaced by the SGSC, as illustrated in Fig. 1, the SGSC is responsible for controlling the stator terminal voltage, as well as the DC-link [25].

In the series-DFIG scheme presented in Fig. 1, the SGSC is coupled to the grid by a series transformer and the DFIG operational principles remain the same. As the current flowing through the SGSC and through the stator machine are the same, or proportional to the series transformer relation, the rotor power flow is controlled by the voltage at the SGSC, given by

$$P = U_{\text{series}d} \times I_{sd} - U_{\text{series}q} \times I_{sq} \tag{1}$$

where $U_{\text{series}d}$ and $U_{\text{series}q}$ are the direct and quadrature components of the voltage induced by the transformer connecting the SGSC, and I_{sd} and I_{sq} are the direct and quadrature components of the stator current.

Considering unbalanced operation conditions, the series-DFIG controls can be separated in positive and negative sequences. The controls applied to the positive sequence variables have the objective to maintain the main functions of the DFIG, controlling the active and reactive power output and the dc link voltage. In this paper these controls have the same objective of the positive sequence controls presented in [25–27]. For the negative sequence control, however, it is proposed a new control methodology. While the negative-sequence controls proposed for the series-DFIG focus only on regulating the output voltage of SGSC for maintaining balanced voltages at the machine stator, in this paper it is proposed to inject an unbalanced current into the grid to compensate the voltage unbalance at the PCC. Although this objective has been used for the conventional DFIG configuration, the series-DFIG presents a better performance for such task, once the consequences of the injection of unbalanced currents can be compensated by applying an adequate voltage at the machine stator, using the SGSC. Besides, the series-DFIG scheme allows improving the voltage ride through capability [23].

To sum up, in the control proposed in this paper, the negative sequence control of the RSC has the objective of injecting a negative sequence current through the machine, and the SGSC has the objective of imposing a voltage to the machine stator to minimize the torque oscillations produced by the negative sequence currents flowing through the machine. The models of the series converter and the machine are following described.

2.1. SGSC model

The SGSC is modelled as illustrated in the three-phase diagram of Fig. 2. A RC filter is connected in parallel to the L_c inductance to reduce the high-frequency distortions present in the output of the three-phase IGBT bridge converter. The equivalent circuit shown in Fig. 2(b) allows calculating the voltage in the series transformer (U_{series}) according to the voltage inserted by the IGBT bridge converter (U_{sc}) and to the RLC values. It is worth noting in Fig. 2(a), the series transformer is delta connected and the RC filter is star connected.

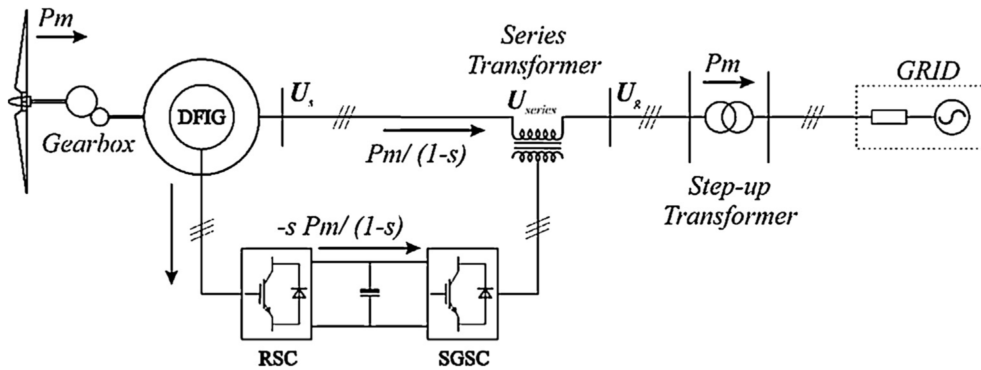

Fig. 1. Series-DFIG scheme.

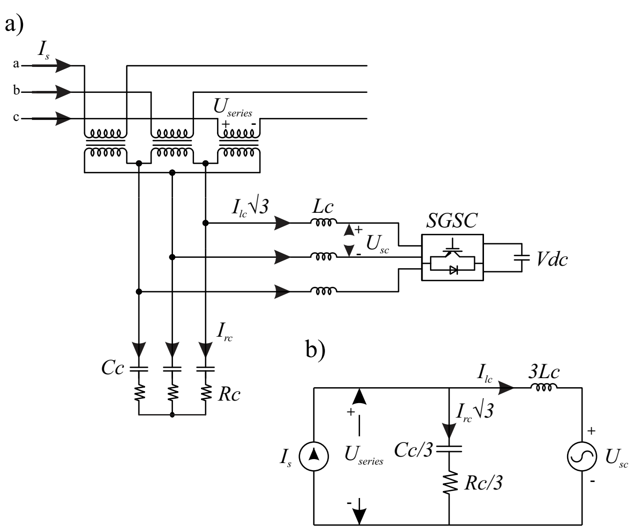

Fig. 2. (a) SGSC three-phase scheme. (b) SGSC equivalent circuit.

The compensation of unbalanced currents by the series-DFIG is implemented based on the machine symmetrical components model, which is following presented.

2.2. Asynchronous machine dynamic model

The *dq* model is frequently used for modelling the wound asynchronous machine. The equations in the *abc* frame and the *dq* transformations can be obtained in [28]. Fig. 3 illustrates the *T* equivalent circuit of the DFIG in the positive sequence synchronous reference frame (dq)+.

In Fig. 3, ω_1 is the synchronous frequency, ω_r is the angular speed of the rotor converted into electrical frequency and $(\omega_1 - \omega_r)$ is the slip frequency. L_m is the magnetizing inductance, $L_{\sigma s}$ ($L_{\sigma r}$) the stator (rotor) leakage inductance, and R_s (R_r) the stator (rotor) resistance. $U^+_{sdq}\left(U^+_{rdq}\right)$, $I^+_{sdq}\left(I^+_{rdq}\right)$ and $\Psi^+_{sdq}\left(\Psi^+_{rdq}\right)$ are the stator (rotor) voltage, current and flux referred to the synchronous reference frame.

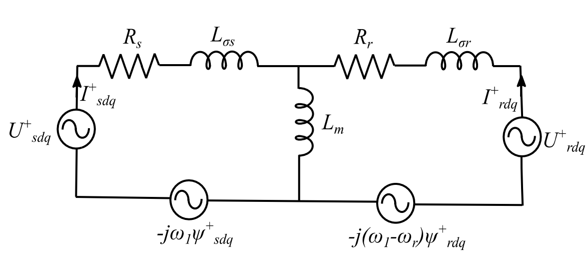

Fig. 3. DFIG equivalent circuit in the $(dq)^+$ reference frame.

According to the equivalent circuit of the DFIG in the positive sequence synchronous reference frame, represented in the equations by the superscript "+", the stator and rotor voltages can be expressed by [29]

$$U^+_{sdq} = \frac{R_s I^+_{sdq} + \mathrm{d}\Psi^+_{sdq}}{\mathrm{d}t + j\omega_1 \Psi^+_{sdq}} \tag{2}$$

$$U^+_{rdq} = \frac{R_r I^+_{rdq} + \mathrm{d}\Psi^+_{rdq}}{\mathrm{d}t + j(\omega_1 - \omega_r)\Psi^+_{rdq}} \tag{3}$$

The fluxes of the stator and of the rotor are given by

$$\Psi^+_{sdq} = L_s I^+_{sdq} + L_m I^+_{rdq} \tag{4}$$

$$\Psi^+_{rdq} = L_m I^+_{sdq} + L_r I^+_{rdq} \tag{5}$$

where

$$L_s = L_m + L_{\sigma s} \tag{6}$$

$$L_r = L_m + L_{\sigma r} \tag{7}$$

Neglecting the impact of R_s losses, the stator voltage can be re-expressed as

$$U^+_{sdq} \approx \frac{\mathrm{d}\left(\Psi^+_{sdq+}\right)}{\mathrm{d}t + j\omega_1\left(\Psi^+_{sdq+}\right)} \tag{8}$$

According to (4), I^+_{sdq} can be expressed:

$$I^+_{sdq} = \frac{\left(\Psi^+_{sdq} - L_m I^+_{rdq}\right)}{L_s} \tag{9}$$

In the equivalent circuit, the electromagnetic power is established by the sum of the power exported from the voltage sources $j\omega_1\Psi^+_{sdq}$ and $j(\omega_1 - \omega_r)\Psi^+_{rdq}$.

$$P_e = -Re\left[j\omega_1\Psi^+_{sdq} \times \hat{I}^+_{sdq} + j(\omega_1 - \omega_r)\Psi^+_{rdq} \times \hat{I}^+_{rdq}\right] \tag{10}$$

Handling the fluxes and currents in the *dq* reference frame as complex numbers, "×" defines the complex product between two complex numbers and "^" the conjugate complex of a complex variable.

Substituting $\hat{I}^+_{sdq}$ and Ψ^+_{rdq} by (9) and (5), respectively, it is possible to simplify (10):

$$P_e = -\omega_r\left(\left(\frac{L_m}{L_s}\right) I_m\left(\Psi^+_{sdq} \times \hat{I}^+_{rdq}\right)\right) \tag{11}$$

From P_e, the electromagnetic torque can be established:

$$T_e = \frac{pP_e}{\omega_r} \tag{12}$$

where p is the number of poles of the asynchronous machine.

The d axis of the dq frame is aligned to phase a of the stator voltage. Hence, the simplification $U^{+}_{sq+} = 0$ is true and can be adopted in the equations.

2.3. Dynamic model of DFIG using symmetrical components

Under unbalanced voltage conditions, the voltages, currents and fluxes of the machine can be expressed by using symmetrical components [7,30]. A variable F is defined to represent vectors expressed in the stator stationary axis $(\alpha\beta)s$ coordinate as [31]

$$\begin{aligned} F_{\alpha\beta}(t) &= F_{\alpha\beta+}(t) + F_{\alpha\beta-}(t) \\ F_{\alpha\beta}(t) &= \left|F_{\alpha\beta+}(t)\right| e^{j(\omega_1 t+\varphi_+)} + \left|F_{\alpha\beta-}(t)\right| e^{-j(\omega_1 t+\varphi_-)} \end{aligned} \tag{13}$$

where the subscripts "+, −" represent the positive and negative sequence components, with "φ_+, φ_-" being their initial phase shifts. In addition, F can be re-expressed in the positive synchronous (dq)+ coordinate and in the negative synchronous (dq)– coordinate, indicated in the equations by the superscripts "+, –", respectively, being ω_1 the synchronous frequency. Thereby, the stator vectors are decomposed into:

$$F^{+}_{dq} = F_{\alpha\beta} e^{-j\omega_1 t} \tag{14}$$

$$F^{-}_{dq} = F_{\alpha\beta} e^{j\omega_1 t} \tag{15}$$

And the rotor vectors, indicated by the superscript r, as

$$F^{+}_{dq} = F^{r}_{\alpha\beta} e^{-j(\omega_1-\omega_r)t} \tag{16}$$

$$F^{-}_{dq} = F^{r}_{\alpha\beta} e^{j(\omega_1-\omega_r)t} \tag{17}$$

The stator/rotor equations can be rewritten in terms of their positive/negative sequence components in the (dq)+ frame. The stator reference frame, expressed by the subscript s, rotates at the frequency of ω_1, and the rotor reference frame, expressed by the subscript r, rotates at the frequency of $(\omega_1 - \omega_r)$,

$$\begin{aligned} F^{+}_{sdq} &= F^{+}_{sdq+} + F^{+}_{sdq-} \\ F^{+}_{sdq} &= F^{+}_{sdq+} + F^{-}_{sdq-} e^{-j2\omega_1 t} \end{aligned} \tag{18}$$

$$\begin{aligned} F^{+}_{rdq} &= F^{+}_{rdq+} + F^{+}_{rdq-} \\ F^{+}_{rdq} &= F^{+}_{rdq+} + F^{-}_{rdq-} e^{-j2\omega_1 t} \end{aligned} \tag{19}$$

The stator voltage can be rewritten in the following decomposed form:

$$\begin{aligned} U^{+}_{sdq} &\approx \mathrm{d}\left(\Psi^{+}_{sdq+} + \Psi^{-}_{sdq-} e^{-j2\omega_1 t}\right)/\mathrm{d}t + j\omega_1\left(\Psi^{+}_{sdq+} + \Psi^{-}_{sdq-} e^{-j2\omega_1 t}\right) \\ U^{+}_{sdq} &\approx j\omega_1\left(\Psi^{+}_{sdq+} - \Psi^{-}_{sdq-} e^{-j2\omega_1 t}\right) \end{aligned} \tag{20}$$

Rewriting the stator current in terms of the positive/negative sequence components:

$$I^{+}_{sdq} = \left(\Psi^{+}_{sdq+} + \Psi^{-}_{sdq-} e^{-j2\omega_1 t}\right)/L_s - L_m(I^{+}_{sdq+} + I^{-}_{sdq-} e^{-j2\omega_1 t})/L_s \tag{21}$$

The electromagnetic power can be decomposed into a continuous component plus pulsating components with frequency of $2\omega_1$. To achieve this decomposition the following equations for the stator flux and rotor current must be applied in (11):

$$\Psi^{+}_{sdq} = \Psi^{+}_{sdq+} + \Psi^{-}_{sdq-} e^{-j2\omega_1 t} \tag{22}$$

where the term $e^{-j2\omega_1 t}$ can be rewritten in the sin/cos form:

$$\Psi^{+}_{sdq} = \Psi^{+}_{sdq+} + \Psi^{-}_{sdq-}(\cos(2\omega_1 t) - j\sin(2\omega_1 t)) \tag{23}$$

The same must be done to the rotor current:

$$I^{+}_{rdq} = I^{+}_{rdq+} + I^{-}_{rdq-}(\cos(2\omega_1 t) - j\sin(2\omega_1 t)) \tag{24}$$

Finally, substituting (23) and (24) in (11), the decomposed form of the electromagnetic power is obtained:

$$P_e = P_{e,dc} + P_{e,\cos(2)}\cos(2\omega_1 t) + P_{e,\sin(2)}\sin(2\omega_1 t) \tag{25}$$

where the subscripts e,dc, and e,sin(2) stand for the dc component and the cosine/sine components at the frequency of $2\omega_1$. The pulsating components are defined by [7]:

$$\begin{bmatrix} P_{e,\cos 2} \\ P_{e,\sin 2} \end{bmatrix} = -\frac{L_m\omega_r}{L_s}\begin{bmatrix} -\Psi^{-}_{sq-} & \Psi^{-}_{sd-} & -\Psi^{+}_{sq+} & \Psi^{+}_{sd+} \\ \Psi^{-}_{sd-} & \Psi^{-}_{sq-} & -\Psi^{+}_{sd+} & -\Psi^{+}_{sq+} \end{bmatrix}\begin{bmatrix} I^{+}_{rd+} \\ I^{+}_{rq+} \\ I^{-}_{rd-} \\ I^{-}_{rq-} \end{bmatrix} \tag{26}$$

By the equations of the asynchronous machine decomposed into positive/negative sequence components, it is possible to establish different objectives of controlling the positive and the negative sequence components of the machine. The proposed control for the reduction of the oscillations in the electromagnetic torque is based on the aforementioned decomposed equations of the electromagnetic power.

3. Proposed control methodology

As already discussed, for controlling the RSC and the SGSC of the series-DFIG scheme, the variables are modelled in the positive and negative sequences and the control is performed independently for each sequence. The controls using the variables in the positive sequence have the objective to maintain the main functions of the DFIG, which are the active and reactive power output and the dc link voltage. The controls using the negative sequence of the variables are responsible for the negative sequence current injection and for minimizing the effect of the unbalanced currents in the machine torque. These controls are following described.

3.1. RSC

The RSC control using the positive sequence variables aims, as a conventional DFIG, controlling the active and reactive output power of the machine. The active power control follows the optimal relationship between the angular speed of the rotor and wind speed, and the reactive power control keeps unitary power factor. Fig. 4 illustrates the diagram block of positive sequence control.

As can be noticed in Fig. 4, the d component of the rotor positive sequence current is responsible for controlling the active output power, while the q component is responsible for controlling the reactive output power. The reference used is based on the stator-voltage orientation.

As seen in Fig. 4, the measured active power of the DFIG ($P(pu)$) is compared with the active power of reference ($P^*(pu)$), obtained of the aerodynamic model of the rotor, the result passes through a proportional integral controller (PI controller) establishing the reference for the direct axis rotor current (Ird^*). To establish the reference for the quadrature axis rotor current (Irq^*), the same process is applied, but using the difference between the measured and reference values of the reactive power of the DFIG ($Q(pu)$, $Q^*(pu)$) as input of the PI controller. The measured rotor current in the dq0 axis (Ird, Irq) is obtained by an abc–dq0 transformation block, and after compared to its reference value and passing through a PI controller, the reference for the positive sequence of the rotor voltage (Urd^*,

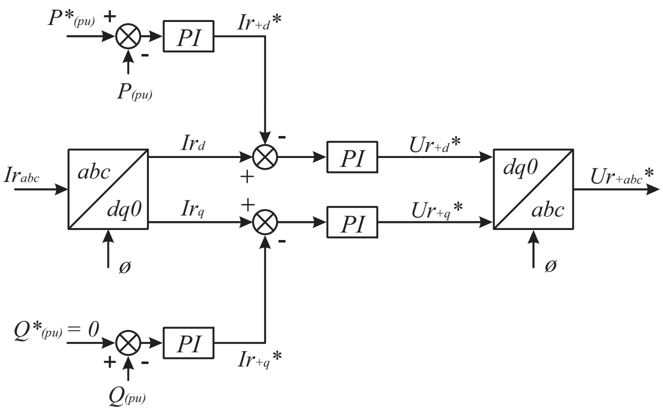

Fig. 4. Block diagram of positive sequence control of the RSC.

*Urq**) is established. A *dq*0–*abc* transformation block establishes the rotor voltage in the *abc* frame.

The RSC negative sequence control is responsible for the negative sequence current injected by the machine stator to compensate the unbalanced grid voltage. To reach this objective, the converter induces an unbalanced voltage at rotor windings, which will be responsible for a negative sequence current in the rotor windings and, therefore, in the stator windings as well. Fig. 5 illustrates the block diagram of the RSC negative sequence control.

As can be seen by Fig. 5, the RSC negative sequence control compares the reference value for negative sequence current of the stator (Is_{-d}^*, Is_{-q}^*) with the measured stator negative sequence current (Is_{-d}, Is_{-q}), which is obtained by a Multiple Second Order Generalized Integrator associated to a Frequency Locked Loop (MSOGI-FLL) [32]. Therefore, applying a PI controller, the reference value for the negative sequence rotor current (Ir_{-d}^*, Ir_{-q}^*) is obtained and, after comparing it to the measured negative sequence rotor current (Ir_{-d}, Ir_{-q}), the error passes through a PI controller to achieve the reference value for the rotor voltage (Ur_{-d}^*, Ur_{-q}^*). The last step is the *dq*0–*abc* transformation block to establish the rotor voltage in the *abc* frame.

The reference for the negative sequence current injection is obtained based on the equivalent negative sequence circuit of a simple transmission network in the synchronous reference frame rotating at $-\omega_1$ [1]. The circuit is illustrated by Fig. 6.

Where, $U_{\text{source}-}$ is the negative sequence voltage before the transmission line, R_L and L_L are the equivalent resistance and

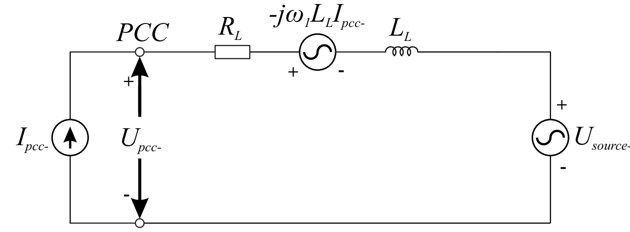

Fig. 6. Equivalent circuit of a simple transmission line rotating at $-\omega_1$.

impedance of the transmission line, I_{pcc-} and U_{pcc-} are the negative sequence current and the negative sequence voltage at the point of common coupling, respectively.

From Fig. 6, the voltage U_{pcc-} can be obtained:

$$U_{pcc-} = \frac{U_{\text{source}-} + R_L I_{pcc-} - j\omega_1 L_L I_{pcc-} + L_L \mathrm{d}I_{pcc-}}{\mathrm{d}t} \tag{27}$$

Representing (27) under steady state in the *dq* frame and neglecting the resistive voltage drop, it can be simplified:

$$\begin{aligned} U_{pcc-d} &= U_{\text{source}-d} + \omega_1 L_L I_{pcc-q} \\ U_{pcc-q} &= U_{\text{source}-q} - \omega_1 L_L I_{pcc-d} \end{aligned} \tag{28}$$

Therefore, to compensate the voltage unbalance in the point of common coupling ($U_{pcc-dq} = 0$), the injected negative sequence current I_{pcc-dq} can be established:

$$\begin{aligned} I_{pcc-q} &= -U_{\text{source}-d}/\omega_1 L_L \\ I_{pcc-d} &= U_{\text{source}-q}/\omega_1 L_L \end{aligned} \tag{29}$$

3.2. SGSC

The control of the SGSC using the positive sequence components is responsible for regulating the DC-Link voltage. However, strategies to increase the fault-ride-through capability can also be implemented [22]. Fig. 7 illustrates the block diagram of the DC-Link voltage control using the SGSC. The control is performed by the *d* component of the SGSC positive sequence voltage. The *q* components of stator and grid voltages are kept aligned and null.

As previously defined, the negative sequence proposed control results in negative sequence currents flowing into the rotor and stator windings. These negative sequence currents produce torque oscillations, which can be eliminated by a specific negative sequence voltage at the SGSC.

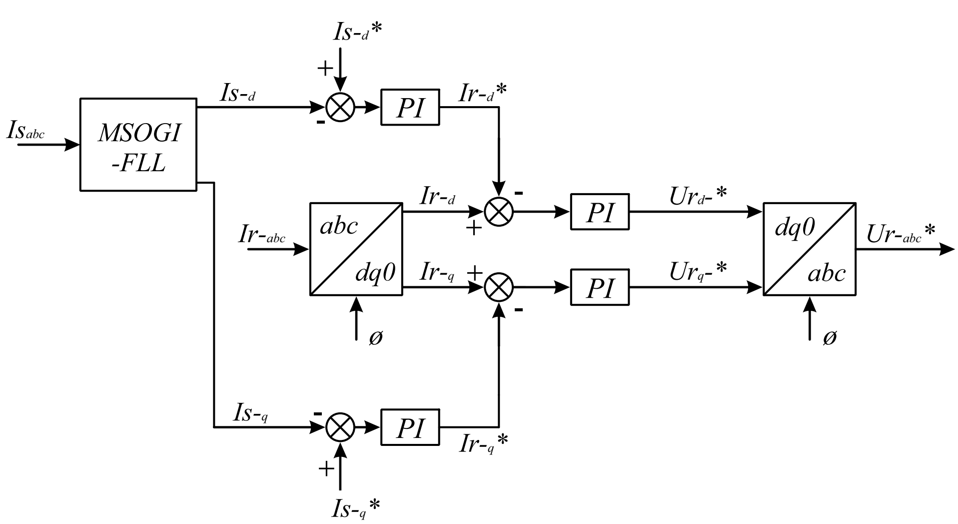

Fig. 5. Block diagram of negative sequence control of the RSC.

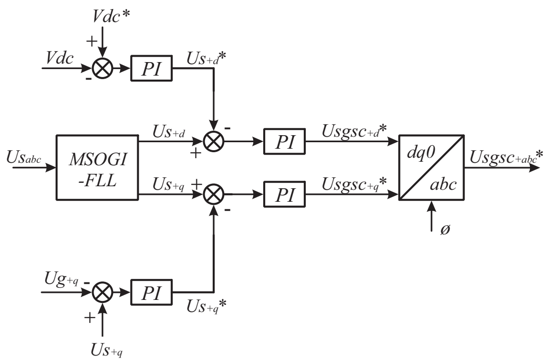

Fig. 7. Block diagram of positive sequence control of the SGSC.

To eliminate the pulsating components of the electromagnetic power, $P_{e,\cos 2}$ and $P_{e,\sin 2}$, the necessary rotor negative sequence current should be obtained by replacing in (26) $P_{e,\cos 2} = 0$ and $P_{e,\sin 2} = 0$, resulting in:

$$I_{rd-}^{-} = \frac{\Psi_{sd-}^{-}}{\Psi_{sq+}^{+}} I_{rq+}^{+} - \frac{\Psi_{sd-}^{-}}{\Psi_{sq+}^{+}} I_{rd+}^{+} \tag{30}$$

$$I_{rq-}^{-} = \frac{\Psi_{sd-}^{-}}{\Psi_{sq+}^{+}} I_{rd+}^{+} + \frac{\Psi_{sq-}^{-}}{\Psi_{sq+}^{+}} I_{rq+}^{+} \tag{31}$$

As the rotor negative sequence current have already been set by the RSC, it is possible to calculate the negative sequence components of the flux Ψ_{sd-}^{-} and Ψ_{sq-}^{-} rearranging (30) and (31). Using the relation between the stator magnetic fluxes and the stator voltages given in (20), it is possible to calculate the stator negative sequence voltage according to the rotor positive/negative sequence current to eliminate the oscillations in the torque:

$$U_{sd-}^{-} = \left(\frac{I_{rd-}^{-} I_{rd+}^{+} - I_{rq-}^{-} I_{rq+}^{+}}{I_{rd+}^{+2} + I_{rq+}^{+2}} \right) U_{sd+}^{+} \tag{32}$$

$$U_{sq-}^{-} = \left(\frac{I_{rq-}^{-} I_{rd+}^{+} + I_{rd-}^{-} I_{rq+}^{+}}{I_{rd+}^{+2} + I_{rq+}^{+2}} \right) U_{sd+}^{+} \tag{33}$$

Appling (32) and (33) as reference for the SGSC negative sequence control the oscillations of torque must be kept in a secure level. Fig. 8 illustrates the block diagram of the SGSC negative sequence control.

In the block diagram presented in Fig. 8, first the negative sequence of the stator voltage at the dq reference frame is obtained. Such voltage is compared to the reference, given by (32) and (33), and the reference of negative sequence voltage for the SGSC is obtained. It is worth noting that when the negative sequence current injection is not required, the SGSC eliminates the negative sequence components of the stator voltage, avoiding any torque oscillations caused by an unbalance at the machine stator.

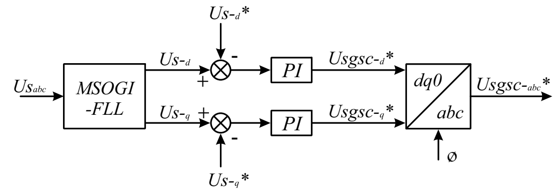

Fig. 8. Block diagram of 0 negative sequence control of the SGSC.

Table 1
DFIG Data.

	DFIG data	
Asynchronous generator	Rated power	2 MVA
	Rated voltage/frequency	575 V/60 Hz
	R_s	0.023 Ω
	R_r	0.016 Ω
	L_{ls}	0.18 H
	L_{lr}	0.16 H
	Inertia constant	0.685 s
	Pair of poles	3
SGSC	L_c	0.001 H
	C_c	0.5 Ω
	R_c	0.012 F
DC link	C_{dc}	0.3 F

4. Validation of the proposed control strategy

Simulations of the proposed control strategies for DFIG based on a series grid side converter scheme are conducted by using Matlab/Simulink. The test system is composed by the series-DFIG, which is connected to the point of common coupling (PCC) by a $Y - \Delta$ transformer. A load is also connected to the PCC. A 50 km π-Line connects the PCC to the 120 kV system, which is composed by a step up transformer, a mutual impedance and a 120 kV controlled voltage source. A grounding transformer is also connected to the 25 kV section to avoid zero-sequence currents flowing in the grid. The proposed system is illustrated in Fig. 9. The DFIG rated power is 2 MVA. Its parameters are given in Table 1.

In the simulations, the unbalance level is represented by the voltage unbalance factor (VUF). This index is calculated by the ratio of the negative sequence voltage with to the positive sequence voltage by [2]:

$$\text{VUF}(\%) = \frac{V_-}{V_+}.100 \tag{34}$$

V_+ and V_- are the positive and negative sequence voltages, respectively.

A VUF of 6% is imposed at the 120 kV controlled voltage source. The aim of the DFIG negative sequence injection is to compensate the voltage unbalance in the point of common coupling avoiding also the unbalance effect at the load. The operational point of the turbine for the first simulation is $\omega_r = 0.93$ p.u. and $T_m = 0.86$ p.u.

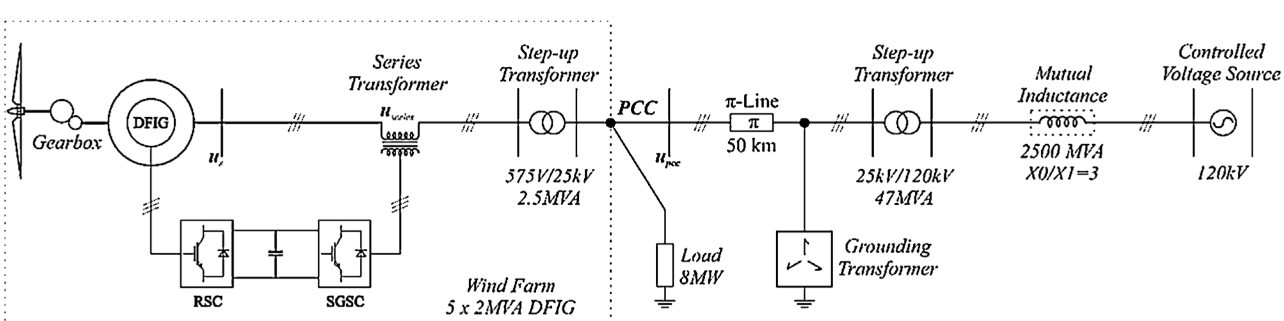

Fig. 9. Test power system configuration with DFIG.

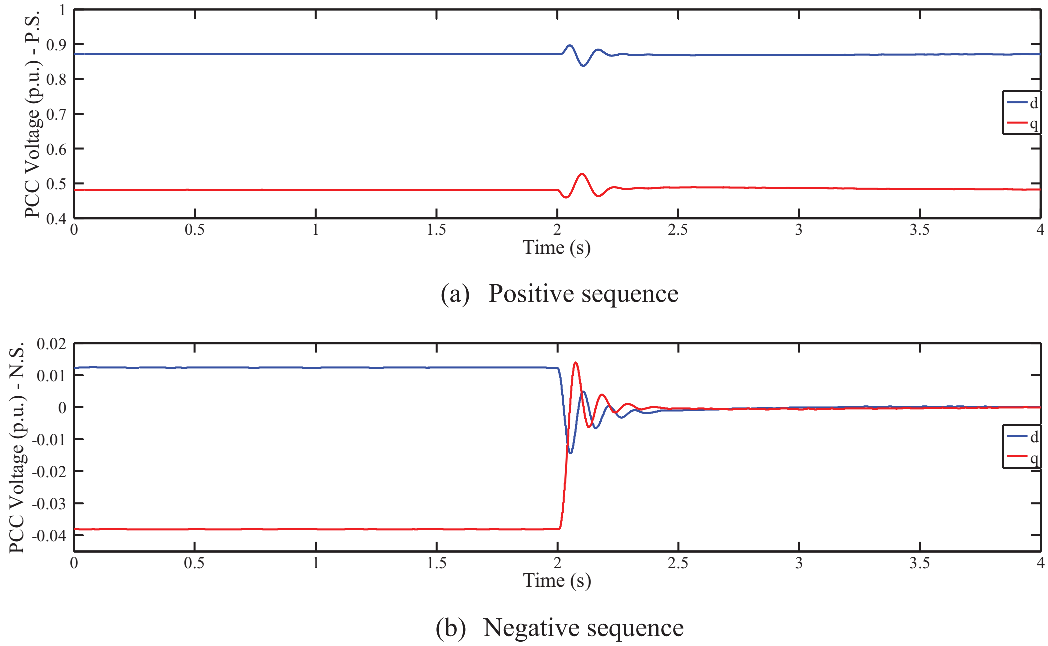

Fig. 10. PCC voltage (p.u.)—(a) positive sequence, (b) negative sequence.

Fig. 10 illustrates the PCC voltage with the unbalance control disabled and enabled. The results are divided in 2 different periods as following described:

- First period (from 0 to 2 s). The negative sequence controls are disabled.
- Second period (from 2 to 4 s). RSC and SGSC negative sequence controls enabled.

As seen in Fig. 10, in the first period, as the negative sequence controls were disabled, the PCC present a VUF of 4%. This unbalance was dramatically reduced to almost zero by means of the negative sequence current injection. The *d* component of the *dq*0 frame is aligned with the stator voltage. Due to the impedance of the 575 V/25 kV step up transformer the PCC voltage is misaligned with the stator voltage.

The load is affected by the voltage unbalance at the PCC, as shown in Fig. 11. As the DFIG negative sequence current injection control compensates the unbalance at the PCC, the negative sequence load current component is reduced. As the compensation control is pretty effective, the load current unbalance is also almost entirely eliminated, thus, avoiding any consequence of the voltage unbalance at the load.

The stator current is responsible for compensating the voltage unbalance at the PCC. Fig. 12 shows, until 2 s, the negative sequence component of the stator current caused by the unbalanced voltage at the stator terminal. After that, the RSC negative sequence control injects a negative sequence current in order to reduce the

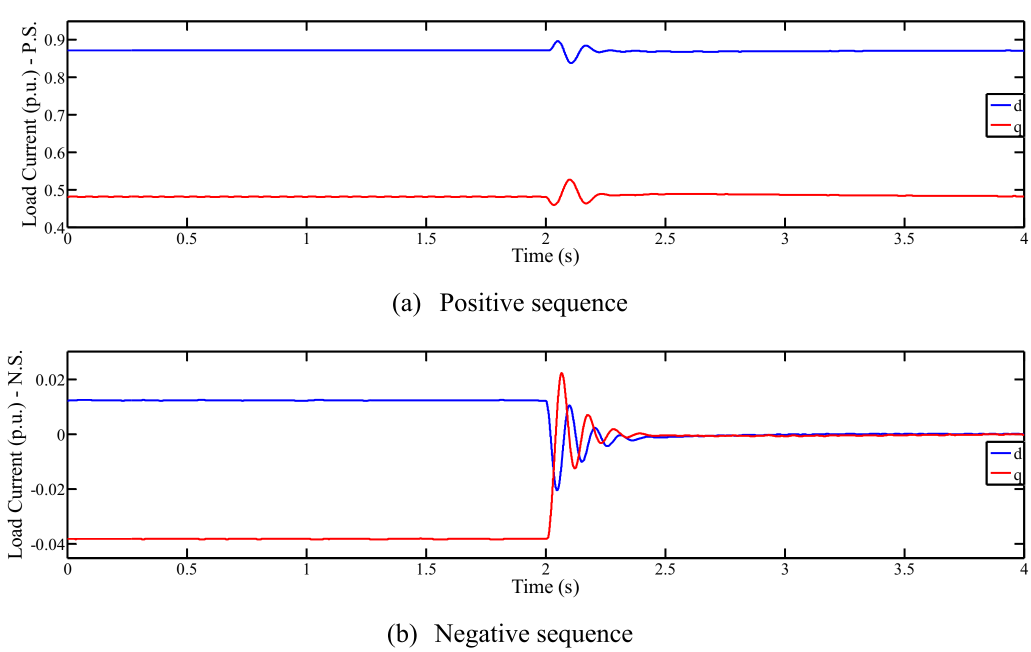

Fig. 11. Load current (p.u.)—(a) positive sequence, (b) negative sequence.

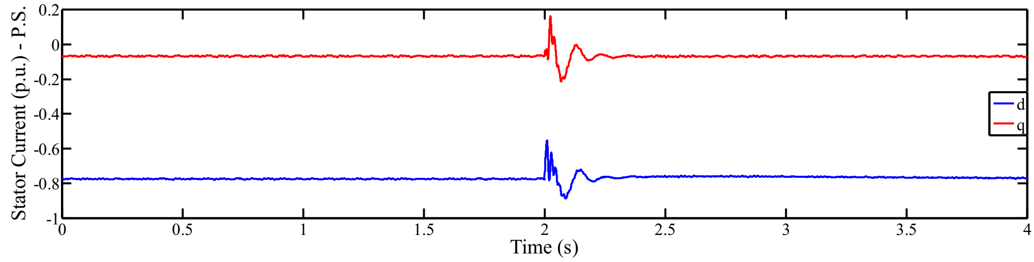

(a) Positive sequence

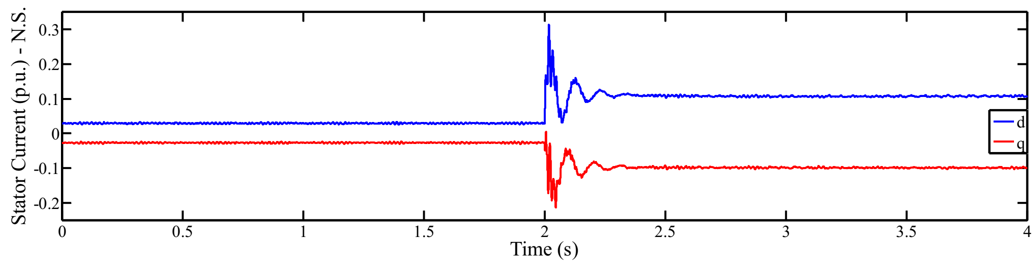

(b) Negative sequence

Fig. 12. Stator current (p.u.)—(a) positive sequence, (b) negative sequence.

unbalance at the PCC. In this case the negative sequence current reached the values of 0.14 p.u. It is worth to mention that the line impedance value used in the simulation associated to the source VUF were defined to need a negative sequence current injection, which required the entire converters power capability.

Fig. 13 illustrates the voltage at the stator terminals. In the first period, VUF is exactly the same of the PCC. In the second period, the SGSC control induces a series voltage, resulting in a stator voltage that eliminates the oscillations in the electromagnetic torque, even if the machine is injecting a negative sequence current from its stator.

Fig. 14(a) presents the electromagnetic torque. In the first period, the oscillations are caused by the unbalanced voltage at the machine stator. In the second period the proposed negative sequence control for the SGSC is shown effective and the oscillations at the frequency $2\omega_1$ is almost eliminated.

As seen in Fig. 14(b), the DFIG stator active power is 0.86 p.u and its reactive power is almost zero. In the first period the SGSC positive sequence control just exchanges the rotor power with the grid. In this case the rotor absorbs 0.12 p.u. of active power from the grid, which means that the total active power of the DFIG is 0.76 p.u. In the second period the SGSC also absorbs active power for the negative sequence controls and its power reaches the limit of 0.3 p.u.

The efficiency of the proposed control for different angles of the injected negative sequence stator current is evaluated by varying

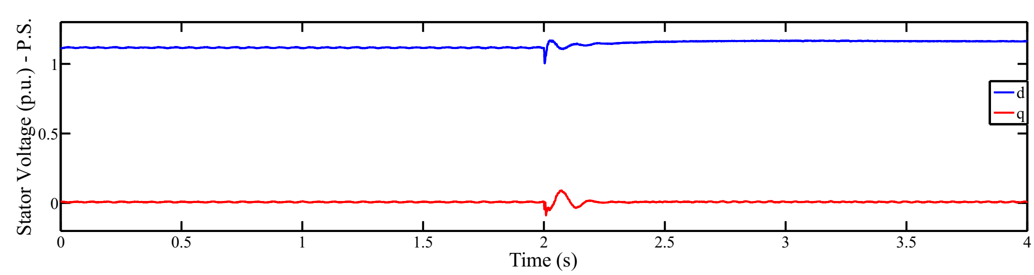

(a) Positive sequence

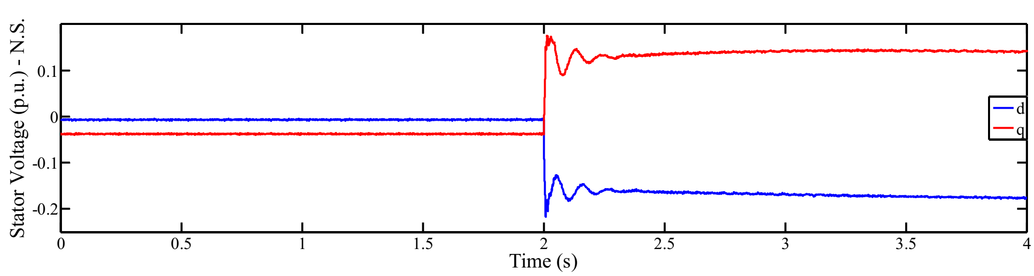

(b) Negative sequence

Fig. 13. Stator voltage (p.u.)—(a) positive sequence, (b) negative sequence.

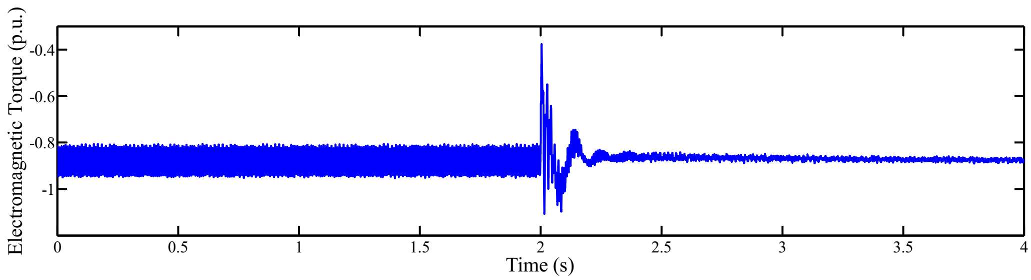

(a) Electromagnetic torque

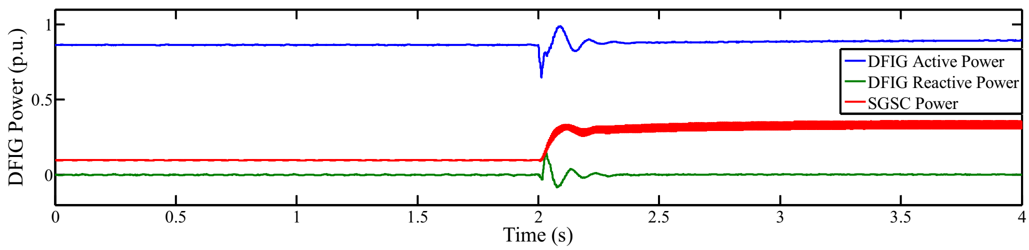

(b) DFIG power

Fig. 14. (a) Electromagnetic torque, (b) DFIG power.

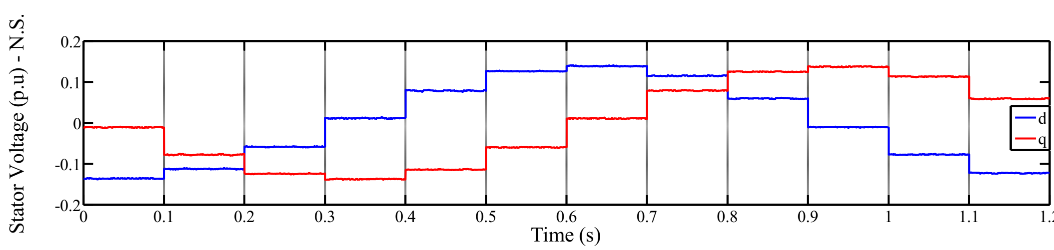

(a) Stator negative sequence voltage

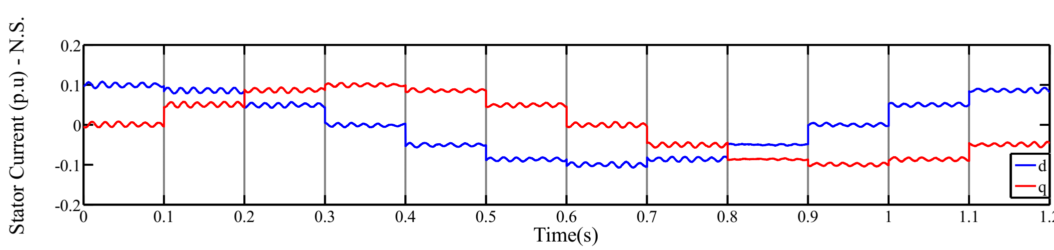

(b) Stator negative sequence current

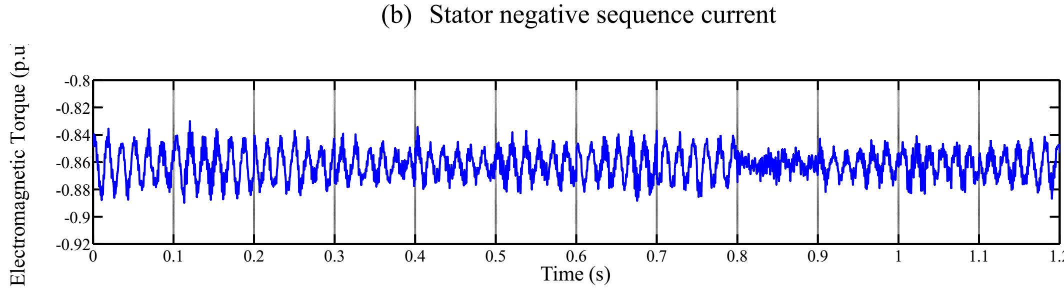

(c) Electromagnetic torque

Fig. 15. Results—current angle validation. (a) Stator negative sequence voltage (b) stator negative sequence current (c) electromagnetic torque.

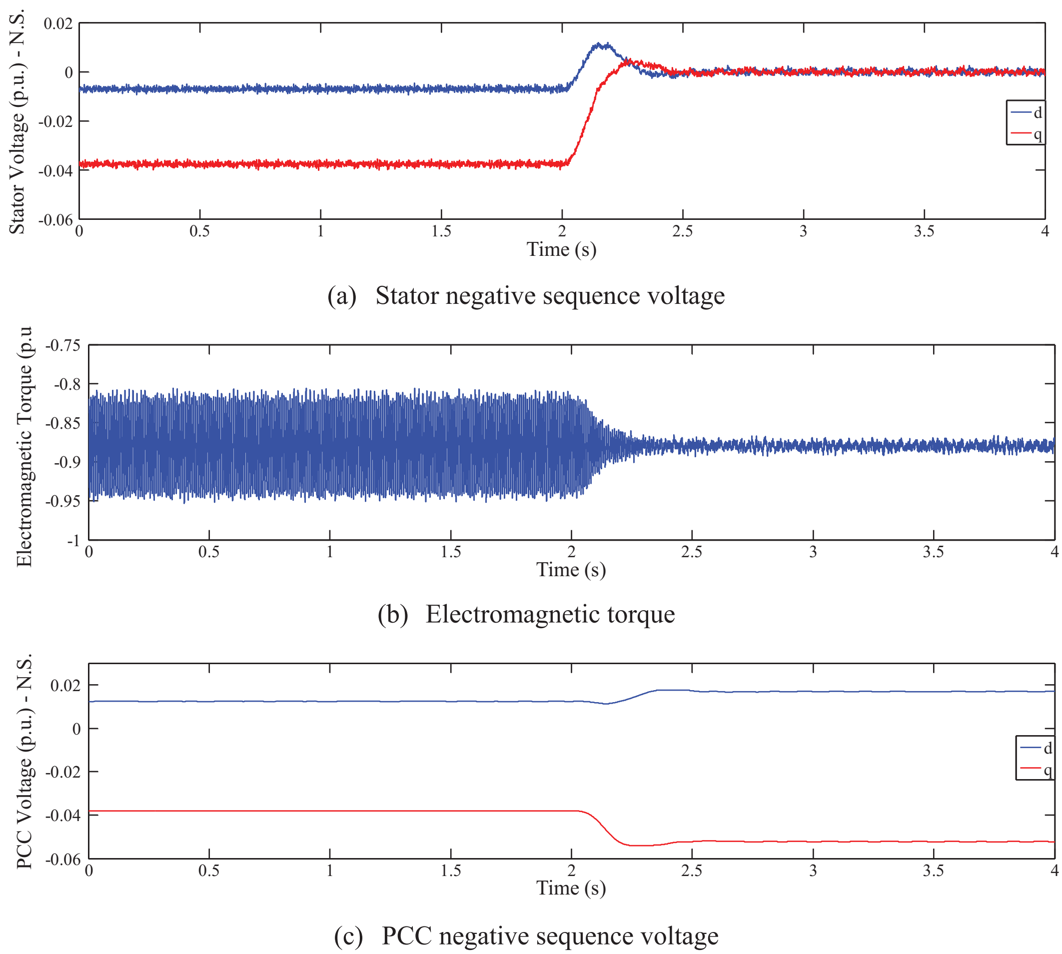

Fig. 16. Stator voltage unbalance compensation (a) stator negative sequence voltage (b) electromagnetic torque (c) PCC negative sequence voltage.

the grid conditions. During simulations, the grid voltage unbalance magnitude is kept constant, but its angle is varied from 0 to 360°, considering steps of 20°. Fig. 15 illustrates the results.

According to Fig. 15, the control was effective for all different angles of stator current. The SGSC control changes the stator negative sequence voltage according to the injected negative sequence current avoiding the increase of the oscillation in the electromagnetic torque.

5. Discussion

Compared to the previous studies with the series-DFIG scheme [25–27], the main advantage of the proposed methodology is to use the potential of this scheme not only to compensate the effects of the voltage unbalance at the machine operation, but also to improve the voltage unbalance level at the grid. In [25–27] the objective is to keep the stator voltage balanced under grid unbalance voltages. In order to compare the results, a simulation using only the negative sequence control of the SGSC with the objective to apply a voltage to compensate the grid unbalanced voltage at the machine stator is run. In the simulation, the series-DFIG is at the same operation point as the operation point used in the validation studies in this paper.

Fig. 16(a) presents the voltage at the machine stator. As can be seen, after the negative sequence control is enabled, the SGSC is able to balance the voltage applied to the stator. After the voltage at the stator is balanced, the torque oscillations are reduced, as can be seen in Fig. 16(b). The balanced machine operation reduces the negative sequence currents of the grid, however, it is not substantial to improve the voltage unbalance at the PCC, as can be seen in Fig. 16(c). The use of the methodology proposed in this paper, however, is capable of eliminating the voltage unbalance, as can be seen in Fig. 10.

6. Conclusion

In this paper, it has been proposed a control methodology for the series-DFIG scheme for compensating the effects of voltage unbalance at the machine and the voltage unbalance at the PCC. As the results confirmed, the proposed methodology has succeed in improving the grid voltage unbalance without compromising the machine operation.

Such task was possible due to the connection in series of the grid side converter, which allows imposing a specific voltage at the machine stator to compensate the effects of the negative sequence current injected by the machine on torque oscillations. As a result, the use of the DFIG scheme based in a series converter using the proposed control methodology can improve the penetration of the DFIG wind turbines in weak grids subjected to voltage unbalance, avoiding the propagation of the unbalance to the loads connected next to the PCC. Additionally, it is worth to highlight that other works have already demonstrated that the series-DFIG operation under grid faults have also presented good performance. As a consequence, this configuration presents a high potential to comply with more restrictive grid codes, requiring more support from the wind farm to the grid operation.

Acknowledgments

The authors gratefully acknowledge the financial support from the Brazilian government via FAPESP (State of Sao Paulo Research Foundation), CNPq (National Council for Scientific and Technological Development) and CAPES (Coordination for the Improvement of Higher Level Personnel).

References

[1] Y. Wang, L. Xu, B.W. Williams, Compensation of network voltage unbalance using doubly fed induction generator-based wind farms, IET Renew. Power Gener. 3 (2009) 12, http://dx.doi.org/10.1049/iet-rpg:20080007.
[2] A. von Jouanne, B. Banerjee, Assessment of voltage unbalance, IEEE Trans. Power Delivery 16 (2001) 782–790, http://dx.doi.org/10.1109/61.956770.
[3] ANSI/NEMA NEMA, Standards Publication MG1-2009: Motors and Generators, 2009.
[4] E.C. Quispe, X.M. Lopez-Fernandez, A.M.S. Mendes, A.J. Marques Cardoso, J.A. Palacios, Experimental study of the effect of positive sequence voltage on the derating of induction motors under voltage unbalance, in: 2011 IEEE Int. Electr. Mach. Drives Conf., IEEE, 2011, pp. 908–912, http://dx.doi.org/10.1109/IEMDC.2011.5994936.
[5] J. Kearney, Grid Voltage Unbalance and the Integration of DFIG's, 2013, ⟨http://arrow.dit.ie/engdoc/56⟩ (accessed November 12, 2015) (Doctoral).
[6] M. Kiani, Effects of voltage unbalance and system harmonics on the performance of doubly fed induction wind generators, IEEE Trans. Ind. Appl. 46 (2010) 562–568, http://dx.doi.org/10.1109/TIA. 2010.2041087.
[7] H. Xu, J. Hu, Y. He, Integrated modeling and enhanced control of DFIG under unbalanced and distorted grid voltage conditions, IEEE Trans. Energy Convers. 27 (2012) 725–736, http://dx.doi.org/10.1109/TEC. 2012.2199495.
[8] T.K.A. Brekken, N. Mohan, Control of a doubly fed induction wind generator under unbalanced grid voltage conditions, IEEE Trans. Energy Convers. 22 (2007) 129–135, http://dx.doi.org/10.1109/TEC. 2006.889550.
[9] Y. Song, H. Nian, Modularized control strategy and performance analysis of DFIG system under unbalanced and harmonic grid voltage, IEEE Trans. Power Electron. 30 (2015) 4831–4842, http://dx.doi.org/10.1109/TPEL. 2014.2366494.
[10] P. Cheng, H. Nian, Collaborative control of DFIG system during network unbalance using reduced-order generalized integrators, IEEE Trans. Energy Convers. 30 (2015) 453–464, http://dx.doi.org/10.1109/TEC. 2014.2363671.
[11] P.-H. Huang, M.S. El Moursi, S.A. Hasen, Novel fault ride-through scheme and control strategy for doubly fed induction generator-based wind turbine, IEEE Trans. Energy Convers. 30 (2015) 635–645, http://dx.doi.org/10.1109/TEC.2014.2367113.
[12] H. Fathabadi, Control of a DFIG-based wind energy conversion system operating under harmonically distorted unbalanced grid voltage along with nonsinusoidal rotor injection conditions, Energy Convers. Manage. 84 (2014) 60–72, http://dx.doi.org/10.1016/j.enconman.2014.03.078.
[13] M. Farshadnia, S.A. Taher, Current-based direct power control of a DFIG under unbalanced grid voltage, Int. J. Electr. Power Energy Syst. 62 (2014) 571–582, http://dx.doi.org/10.1016/j.ijepes.2014.05.009.
[14] L. Xu, Y. Wang, Dynamic modeling and control of DFIG-based wind turbines under unbalanced network conditions, IEEE Trans. Power Syst. 22 (2007) 314–323, http://dx.doi.org/10.1109/TPWRS. 2006.889113.
[15] L. Fan, H. Yin, Z. Miao, A novel control scheme for DFIG-based wind energy systems under unbalanced grid conditions, Electr. Power Syst. Res. 81 (2011) 254–262, http://dx.doi.org/10.1016/j.epsr.2010.08.011.
[16] J. Hu, Y. He, L. Xu, Improved rotor current control of wind turbine driven doubly-fed induction generators during network voltage unbalance, Electr. Power Syst. Res. 80 (2010) 847–856, http://dx.doi.org/10.1016/j.epsr.2009.12.010.
[17] J. Hu, Y. He, Modeling and enhanced control of DFIG under unbalanced grid voltage conditions, Electr. Power Syst. Res. 79 (2009) 273–281, http://dx.doi.org/10.1016/j.epsr.2008.06.017.
[18] E. Tremblay, A. Chandra, P.J. Lagace, Grid-side converter control of DFIG wind turbines to enhance power quality of distribution network, in: 2006 IEEE Power Eng. Soc. Gen. Meet., IEEE, 2006, p. 6, http://dx.doi.org/10.1109/PES.2006.1709488.
[19] R. Pena, R. Cardenas, E. Escobar, J. Clare, P. Wheeler, Control strategy for a doubly-fed induction generator feeding an unbalanced grid or stand-alone load, Electr. Power Syst. Res. 79 (2009) 355–364, http://dx.doi.org/10.1016/j.epsr.2008.07.005.
[20] J. Hu, H. Xu, Y. He, Coordinated control of DFIG's RSC and GSC under generalized unbalanced and distorted grid voltage conditions, IEEE Trans. Ind. Electron. 60 (2013) 2808–2819, http://dx.doi.org/10.1109/TIE. 2012.2217718.
[21] L. Fan, Z. Miao, Modeling and Analysis of Doubly Fed Induction GeneratorWind Energy Systems, Elsevier, Amsterdam, 2015.
[22] C.K.W. Schumacher, Active damping of flux oscillations in doublyfed ac machines using dynamic variation of the system's structure, in: Ninth Eur. Conf. Power Electron. Appl., Graz, Austria, 2001.
[23] P.S. Flannery, G. Venkataramanan, A Fault tolerant doubly fed induction generator wind turbine using a parallel grid side rectifier and series grid side converter, IEEE Trans. Power Electron. 23 (2008) 1126–1135, http://dx.doi.org/10.1109/TPEL. 2008.921179.
[24] Y. Liao, H. Li, J. Yao, K. Zhuang, Operation and control of a grid-connected DFIG-based wind turbine with series grid-side converter during network unbalance, Electr. Power Syst. Res. 81 (2011) 228–236, http://dx.doi.org/10.1016/j.epsr.2010.09.002.
[25] B. Singh, V. Emmoji, S.N. Singh, I. Erlich, Performance evaluation of new series connected grid-side converter of doubly-fed induction generator, in: 2008 Jt. Int. Conf. Power Syst. Technol. IEEE Power India Conf., IEEE, 2008, pp. 1–8, http://dx.doi.org/10.1109/ICPST.2008.4745315.
[26] N.G. Jayanti, M. Basu, K. Gaughan, M.F. Conlon, A new configuration and control of doubly fed induction generator (UPQC-WG), in: 2008 34th Annu. Conf. IEEE Ind. Electron., IEEE, 2008, pp. 2094–2099, http://dx.doi.org/10.1109/IECON.2008.4758280.
[27] J.R. Massing, H. Pinheiro, Design and control of doubly-fed induction generators with series grid-side converter, in: 2008 34th Annu. Conf. IEEE Ind. Electron., IEEE, 2008, pp. 139–145, http://dx.doi.org/10.1109/IECON.2008.4757942.
[28] P.C. Krause, O. Wasynczuk, S. Sudhoff, Analysis of Electric Machinery and Drive Systems, second ed., John Wiley & Sons, New York, United States, 2002.
[29] P. Kundur, Power System Stability and Control, McGraw-Hill, New York, United States, 1994.
[30] G. Abad, J. López, M. Rodríguez, L. Marroyo, G. Iwanski, Doubly Fed Induction Machine: Modeling and Control for Wind Energy Generation, first ed., John Wiley & Sons, New York, United States, 2011.
[31] J.C. Das, Power System Analysis: Short-Circuit Load Flow and Harmonics, second ed., CRC Press, Boca Raton, Forida, United States, 2011.
[32] P. Rodriguez, A. Luna, I. Candela, R. Mujal, R. Teodorescu, F. Blaabjerg, Multiresonant frequency-locked loop for grid synchronization of power converters under distorted grid conditions, IEEE Trans. Ind. Electron. 58 (2011) 127–138, http://dx.doi.org/10.1109/TIE. 2010.2042420.